Available online at www.sciencedirect.com
SCIENCE DIRECT
Journal of Molecular Structure 744–747 (2005) 3–17
Journal of MOLECULAR STRUCTURE
www.elsevier.com/locate/molstruc

Conformational stability from variable temperature infrared spectra of krypton and xenon solutions, ab initio calculations, vibrational assignment and r_0 structural parameters of vinylcyclopropane

James R. Durig[a,*], Chao Zheng[a,1], Hamondeh Deeb[a], Gamil A. Guirgis[b]

[a]Department of Chemistry, University of Missouri–Kansas City, Kansas City, MO 64110, USA
[b]Department of Chemistry and Biochemistry, College of Charleston, Charleston, SC 29401, USA

Received 3 November 2004; accepted 22 November 2004
Available online 5 February 2005

Abstract

The infrared spectra (3200–400 cm^{-1}) of krypton and xenon solutions of vinylcyclopropane c-$C_3H_5CH{=}CH_2$, at variable temperatures (−55 to −150 °C) have been recorded. Additionally, the infrared spectra (3200–250 cm^{-1}) of the gas and solid have been recorded. From a comparison of the spectra of the fluid phases with that of the solid, all of the fundamental vibrations of the *trans* conformer have been identified and assigned as well as many of those for the *gauche* form. By utilizing five pairs of fundamentals for these two conformers in the xenon solutions, an enthalpy difference of 415 ± 42 cm^{-1} (4.96 ± 0.50 kJ/mol) has been obtained with the *trans* conformer the more stable form. There is $21 \pm 3\%$ of the *gauche* conformer present at ambient temperature. Results from ab initio calculations show the *cis* rotamer is a transition state. Equilibrium geometries and total energies of both conformers have been determined from ab initio calculations with full electron correlation by the perturbation method to second order as well as by hybrid density functional theory calculations with the B3LYP method using a number of basis sets. The MP2 calculations predict the *trans* conformer to be more stable than the *gauche* form ranging from 358 to 440 cm^{-1} whereas the B3LYP calculations predict significantly larger values between 571 and 616 cm^{-1}. By adjusting ab initio MP2(full)/6-311+G(d,p) predicted structural parameters to fit previously reported rotational constants for the *trans* conformer, adjusted r_0 parameters have been obtained. Comparisons of these parameters to those previously obtained from the microwave and electron diffraction studies are made. Many of the spectroscopic and theoretical results are compared to the corresponding properties for some similar molecules.

Keywords: Vinylcyclopropane; Conformational stability; Ab initio calculations; Structural parameters

1. Introduction

The mono-substituted cyclopropanes have been of interest to structural chemists and physicists for decades, particularly the mono-substituted methylcyclopropanes, c-$C_3H_5CH_2X$, where X = C≡N, C≡CH, CH_3, F, Cl, and Br, since all of them have multiple conformations present at ambient temperature. However, it is not clear what is the major factor or factors that determine which conformer is the most stable form. For example, both cyano [1,2] and ethynyl [3,4] methylcyclopropanes have large amounts of the *cis* conformer present (substituent X over the three-member ring) at ambient temperature whereas for the ethynyl molecule it is the more stable rotamer. The halomethylcyclopropanes [5–12], however, have the *gauche* conformer as the more stable form. Initially, it was suggested [3] that the electronegativity [13] of the substituent on the methylene group was the controlling factor, i.e. substituent with higher electronegativity favors the *cis* form, but our [12] recent determination of the conformational stability of fluoromethylcyclopropane ruled out the electronegativity as the major factor. The cyclopropyl carbonyl compounds, c-C_3H_5CXO, where X = H, F, and

* Corresponding author. Address: Department of Chemistry and Geosciences, University of Missouri–Kansas City, 5100 Rockhill Road, Kansas City, MO 64110-2499, USA. Tel.: +1 816 235 6038; fax: +1 816 235 2290.
E-mail address: durigj@umkc.edu (J.R. Durig).
[1] Taken in part from the thesis of C. Zheng, which will be submitted to the Department of Chemistry of the University of Missouri-Kansas City in partial fulfillment of the PhD degree.

0022-2860/$ - see front matter © 2004 Published by Elsevier B.V.
doi:10.1016/j.molstruc.2004.11.071

Cl are also structurally interesting since they have *cis* (oxygen atom over the three-member ring) and *trans* (halogen atom over the three-member ring) conformers very small enthalpy differences ($\Delta H \approx 100\ cm^{-1}$) with only the chloride having the *cis* conformer the more stable form [14–22]. While the cyclopropylcarboxaldehyde, *c*-C_3H_5—CHO, molecule has *trans* and *cis* conformers [21–23], the isoelectronic vinylcyclopropane molecule, *c*-$C_3H_5CH{=}CH_2$, does not appear to have a stable *cis* form [24–26] although a thorough search for this conformer may not have been made.

There have been several experimental [24–30] and theoretical [31–34] studies of the conformational stability of vinylcyclopropane and it is clear that the most stable conformer is the *trans* form (double bond *trans* to the three-member ring) and there is a second conformer in the fluid phase which has been identified as the *gauche* form (Fig. 1). There have been three experimental determinations of the enthalpy difference between these two conformers with the first one from an electron diffraction investigation [24] with a reported ΔH of $385 \pm 70\ cm^{-1}$ (4.61 ± 0.84 kJ/mol). There were then two Raman investigations which appeared in the same year, and in the first study [25], an enthalpy difference from the temperature dependence of two Raman lines in the spectrum of the gas gave a value of $500 \pm 50\ cm^{-1}$ (5.98 ± 0.60 kJ/mol). In the second study [26], the pair of Raman bands at 1191 and 1203 cm^{-1} were analyzed at five different temperatures from 23 to 85 °C from which an enthalpy value of 1117 ± 91 cal/mol (4.67 ± 0.38 kJ/mol, $391 \pm 32\ cm^{-1}$) was obtained.

As a continuation of our conformational stability studies of mono-substituted cyclopropanes, we recorded variable temperature infrared spectra of krypton and xenon solutions of vinylcyclopropane. We also recorded the infrared spectra of the gas and solid since these spectra do not appear to have been previously published. The Raman spectra of the liquid were recorded from 1500 to 50 cm^{-1} for comparison to that previously published [25,26]. We also carried out MP2(full)/6-311+G(d,p) calculations to obtain the optimized geometries which were combined with the previously reported rotational constants from the two microwave studies [27,28] to obtain the adjusted r_0 parameters [35]. Additional ab initio and density functional theory (DFT) calculations by the B3LYP method have been carried out with a variety of basis sets up to 6–311G(2df,2pd), as well as with diffuse functions, to predict the conformational stabilities. The results of these spectroscopic and theoretical studies are reported herein.

2. Experimental

The sample of vinylcyclopropane was synthesized in two steps as previously reported by Kisiel et al. [28]. First, cyclopropylmethyl ketone was treated with 10 equivalents of toluene-*p*-sulfonic hydrazide and a catalytic amount of toluene-*p*-sulfonic acid in ethanol and refluxed for 1 h. Then the product cyclopropyl carbonyl tosyl hydrozone was reduced with sodium hydride in decaline at 170–180 °C for 3 h. Nitrogen was bubbled through the solution and the volatile vinylcyclopropane was collected in three successive traps maintained at −80 °C. The product was first purified using trap-to-trap technique and then subjected to a low-pressure, low-temperature fractionation column for final purification. The purity of the sample was checked by infrared and NMR spectrometry. The purified sample was kept in the dark at low temperature until it was used.

The mid-infrared spectra of the gas (Fig. 2A) and the annealed solid (Fig. 2B) from 3200 to 250 cm^{-1} were recorded on a Perkin–Elmer model 2000 Fourier transform spectrometer equipped with a nichrome wire source, Ge/CsI beamsplitter and DTGS detector. The spectrum of the gas was obtained with the sample contained in a 12 cm cell equipped with CsI windows. Atmospheric water vapor was removed from the spectrometer chamber by purging with dry nitrogen. For the annealed solid, the spectrum was recorded by depositing a solid sample film onto a CsI substrate cooled by boiling liquid nitrogen and housed in

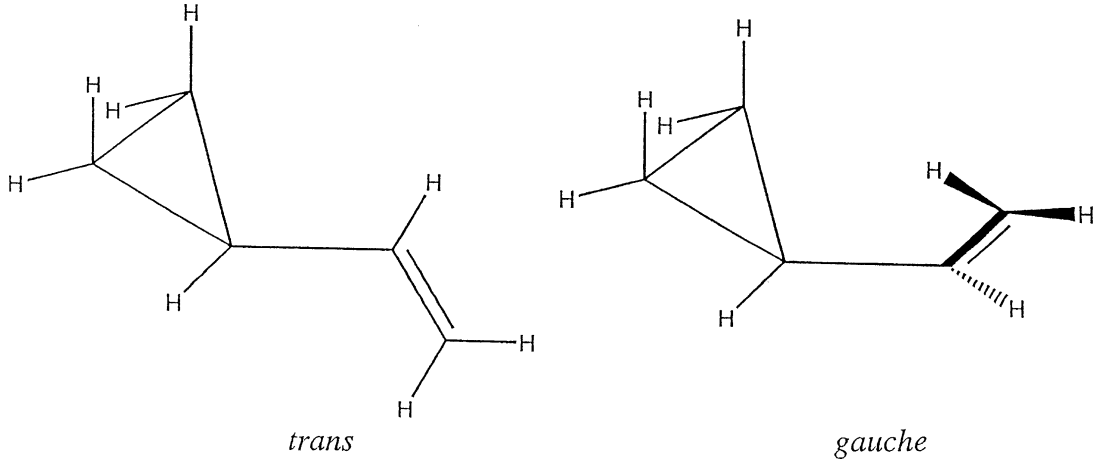

Fig. 1. The *trans* and *gauche* conformers of vinylcyclopropane.

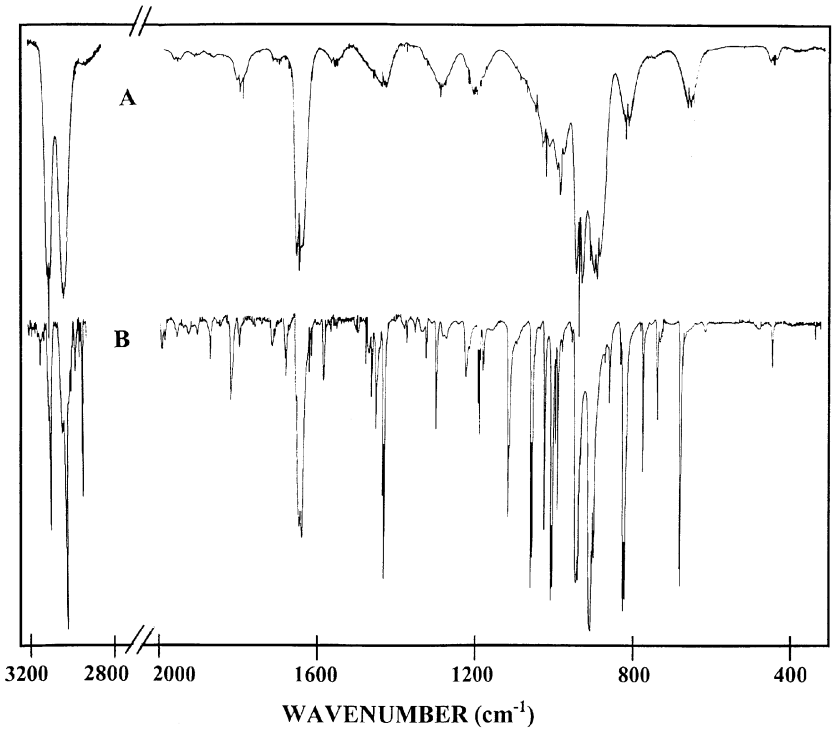

Fig. 2. Infrared spectrum of: (A) gaseous; and (B) polycrystalline solid vinylcyclopropane.

a vacuum cell fitted with CsI windows. The sample was annealed until no further change was observed in the spectrum. Interferograms obtained after 256 scans for the gas sample and reference as well as 128 scans for the amorphous and annealed solid sample and reference were transformed by using a boxcar truncation function with theoretical resolutions of 0.5 and 1.0 cm^{-1}, respectively, for the gaseous and solid samples.

The far infrared spectra of the gas and solid were recorded on the previously described Perkin–Elmer model 2000 spectrometer equipped with a metal grid beamsplitter and a DTGS detector. The gas was contained in a cell with a 12 cm path length and equipped with polyethylene windows. For obtaining the spectra of the solid, the sample was deposited on a Si substrate held at 77 K with boiling liquid nitrogen which was contained in a cryostat cell equipped with polyethylene windows. Normally 256 scans at resolutions of 0.5 and 1.0 cm^{-1} were used for the far infrared spectrum of the gas and the solid, respectively, to give a satisfactory signal-to-noise ratio.

The mid-infrared spectra of the sample dissolved in liquefied krypton (Fig. 3A) and xenon were recorded on a Bruker model IFS-66 Fourier interferometer equipped with a Globar source, Ge/KBr beamsplitter, and DTGS detector. The spectra were recorded at variable temperatures ranging from −55 to −100 °C in krypton solutions as well as −105 to −150 °C in krypton solutions with 100 scans at a resolution of 1.0 cm^{-1}. The temperature studies in these rare gases were carried out in a specially designed cryostat cell, which is composed of a copper cell with a 4 cm path length and wedged silicon windows sealed to the cell with indium gaskets. The temperature was monitored by two Pt thermoresistors and the cell was cooled by boiling liquid nitrogen. The complete cell was connected to a pressure manifold to allow for the filling and evacuation of the cell. After the cell was cooled to the desired temperature, a small amount of sample was condensed into the cell. Next, the pressure manifold and the cell were pressurized with noble gas, which immediately started condensing in the cell, allowing the compound to dissolve.

The observed wavenumbers for the fundamentals of the *trans* and *gauche* conformers are listed in Tables 1 and 2, respectively, along with their predicted values.

3. Theoretical calculations

The LCAO-MO-SCF restricted Hartree–Fock (RHF) calculations were performed with the GAUSSIAN-03 program [36] using Gaussian-type basis functions. The energy minima with respect to nuclear coordinates were obtained by simultaneous relaxation of all geometric parameters consistent with symmetry restrictions using the gradient method of Pulay [37]. A number of basis sets starting from 6-31G(d), increasing to 6-311+G(2df,2pd) were employed at the level of Hartree–Fock, Møller–Plesset perturbation theory to the second order (MP2), and hybrid density functional theory by the B3LYP method to obtain energy differences between the two stable conformers (Table 3). From all levels of calculation conducted in the present

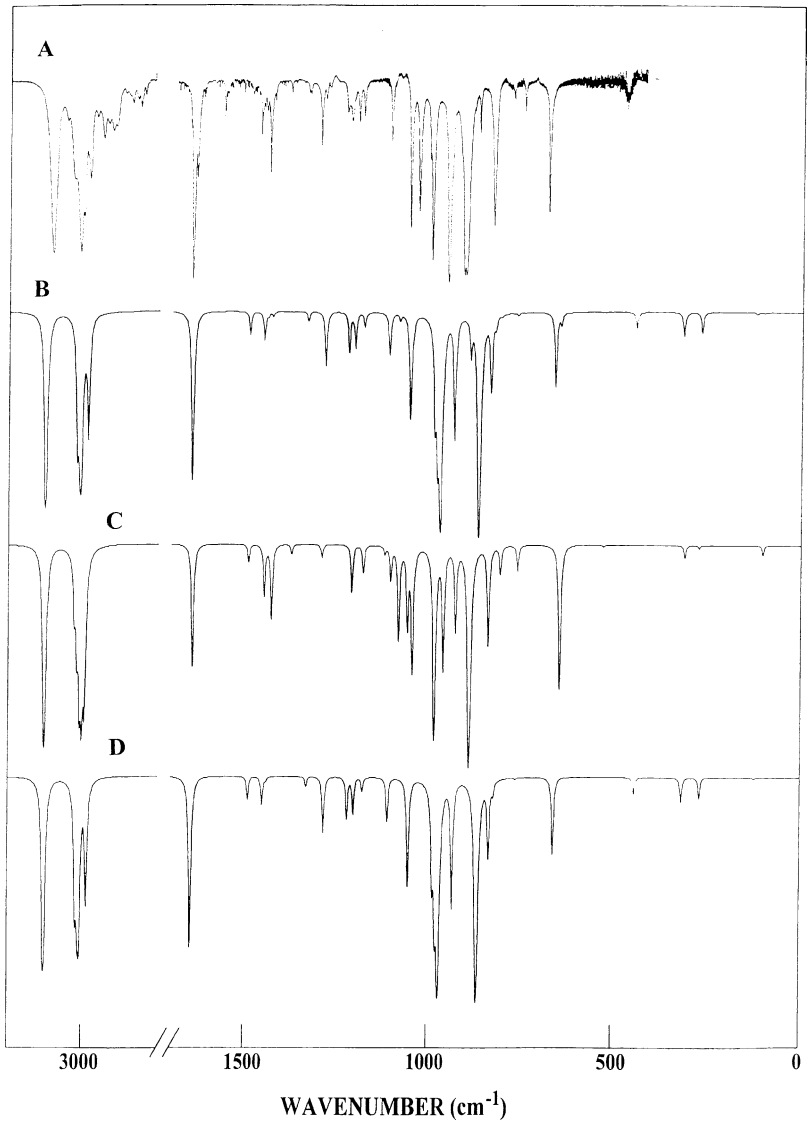

Fig. 3. Infrared spectra of vinylcyclopropane: (A) krypton solution at −130 °C; (B) simulated spectrum, at −130 °C, of a mixture of the two conformers with ΔH of 415 cm^{-1} with the *trans* form more stable; (C) simulated spectrum for pure *gauche* form; (D) simulation spectrum for pure *trans* form.

investigation, the *trans* conformer is always predicted to be the more stable form. The MP2 calculations predict conformational energy differences between 358 and 440 cm^{-1}, whereas B3LYP calculations predict about 50% larger conformational energy differences ranging between 571 and 616 cm^{-1}. Energies of two distinctive transition states, i.e. the *cis* and the *gauche'* conformers were also calculated with the above described methods/basis sets (Table 3).

In order to obtain a more complete description of the nuclear motions involved in the fundamental vibrations of vinylcyclopropane, we have carried out normal a coordinate analysis. The force field in Cartesian coordinates was calculated by the GAUSSIAN-03 program [36] at the MP2(full)/6-31G(d) level. The internal coordinates used to calculate the **G** and **B** matrices are listed along with the structural parameters in Table 4 and the numbering is shown in Fig. 4. By using the **B** matrix, the force field in Cartesian coordinates was converted to a force field in internal coordinates [38] in which the pure ab initio vibrational frequencies were reproduced. Subsequently, scaling factors of 0.88 for the CH stretches, 1.0 for heavy atom bends and torsions and 0.90 for all other modes were used, along with the geometric average of scaling factors for interaction force constants, to obtain the fixed scaled force field and the resultant wavenumbers. A set of symmetry coordinates (Table 5) was used to determine the corresponding potential energy distributions (PEDs). The observed and calculated wavenumbers of the *trans* and *gauche* conformers of vinylcyclopropane, along with the calculated infrared intensities, Raman activities, depolarization ratios and PEDs are given in Tables 1 and 2.

In order to identify the fundamental vibrations for the *trans* and *gauche* conformers of vinylcyclopropane,

Table 1
Observed and calculated frequencies (cm^{-1}) for *trans* vinylcyclopropane

	Vib. No.	Fundamental	Ab initio[a]	Fixed scaled[b]	IR int.[c]	Raman act.[d]	dp Ratio	IR gas	Raman gas[e]	IR Kr[f]	Raman liquid	IR solid	Raman solid[e]	P.E.D.[g]	A[h]	B[h]	C[h]
A′	ν_1	$=CH_2$ antisymmetric stretch	3307	3103	14.5	61.2	0.67	3093	–	3089	–	3087	–	$98S_1$	21	–	79
	ν_2	rCH_2 antisymmetric stretch	3305	3100	11.8	47.1	0.65	3087	–	3080	–	3078	–	$99S_2$	15	–	85
	ν_3	$=CH_2$ symmetric stretch	3216	3017	3.2	127.8	0.11	3020	–	3017	–	3016	–	$94S_3$	78	–	22
	ν_4	rCH stretch	3215	3016	6.2	87.5	0.12	3020	–	3016	–	3016	–	$83S_4$, $14S_5$	8	–	92
	ν_5	rCH_2 symmetric stretch	3208	3010	9.8	91.8	0.06	3010	–	3005	–	2998	–	$85S_5$, $14S_4$	51	–	49
	ν_6	=CH stretch	3185	2988	8.9	43.6	0.39	2987	–	2988	–	2988	–	$93S_6$	1	–	99
	ν_7	C=C stretch	1733	1645	15.4	28.9	0.22	1646	1647	1644	1641	1635/1638	1636	$64S_7$, $14S_9$	99	–	1
	ν_8	rCH_2 deformation	1569	1488	1.2	10.8	0.59	1459	1461	1457	1453	1459	1452	$80S_8$, $13S_{13}$	15	–	85
	ν_9	$=CH_2$ deformation	1515	1437	0.2	24.8	0.36	1437	1437	1441	1430	1427/1431	1433	$63S_9$	0	–	100
	ν_{10}	rCH in-plane bend	1400	1328	0.5	7.5	0.69	1328	1330	1327	1323	1319/1322	1325	$34S_{10}$, $18S_9$, $16S_7$, $12S_{13}$	46	–	54
	ν_{11}	=CH in-plane bend	1350	1281	3.2	8.4	0.41	1294	1296	1292	1293	1293/1295	1295	$64S_{11}$, $13S_{15}$, $10S_7$	36	–	64
	ν_{12}	=C–C stretch	1275	1218	2.3	9.4	0.75	1220	1219	1220	1214	1212/1229	1214	$23S_{12}$,$15S_{18}$,$13S_{15}$, $12S_{10}$,$11S_{19}$	99	–	1
	ν_{13}	Ring breathing	1264	1200	2.0	29.8	0.15	1190	1191	1188	1187	1185/1189	1186	$58S_{13}$, $24S_{10}$	85	–	15
	ν_{14}	rCH_2 wag	1105	1052	2.0	5.2	0.43	1024	–	1023	1022	1018/1021	1023	$85S_{14}$, $13S_{16}$	9	–	91
	ν_{15}	$=CH_2$ wag	1038	985	5.9	1.0	0.55	990	–	993	993	998/1001	989	$42S_{15}$, $17S_{17}$, $16S_{18}$, $12S_{11}$	95	–	5
	ν_{16}	Ring deformation	1005	969	34.3	14.7	0.75	941	–	940	938	934/938	987	$57S_{16}$, $14S_{12}$, $13S_{14}$	91	–	9
	ν_{17}	rCH_2 rock	856	818	0.6	3.2	0.50	819	–	817	816	820/828	821	$38S_{17}$, $19S_{12}$, $17S_{15}$, $16S_{16}$	14	–	86
	ν_{18}	rCH_2 twist	798	758	0.1	5.7	0.59	761	764	762	763	771/773	767	$48S_{18}$, $31S_{17}$	64	–	36
	ν_{19}	C=C–C bend	452	441	0.9	6.4	0.29	446	–	445	452	444	443	$42S_{19}$, $27S_{20}$	88	–	12
	ν_{20}	Ring-C in-plane bend	273	268	1.1	1.1	0.75	273	–	–	276	279/280	284	$58S_{20}$, $37S_{19}$	89	–	11
A″	ν_{21}	rCH_2 antisymmetric stretch	3293	3089	0.1	78.0	0.75	3086		3080	–	3078	–	$100S_{21}$	–	100	–
	ν_{22}	rCH_2 symmetric stretch	3205	3006	13.2	28.0	0.75	3012		3015	–	2998	–	$100S_{22}$	–	100	–
	ν_{23}	rCH_2 deformation	1526	1448	1.5	10.4	0.75	~1456		1454	1453	1448/1448	1445	$100S_{23}$	–	100	–
	ν_{24}	rCH_2 twist	1238	1175	0.7	7.7	0.75	1176		1174	~1175	1171/1182	1175	$44S_{24}$, $46S_{30}$	–	100	–
	ν_{25}	rCH out-of-plane bend	1168	1108	2.4	0.9	0.75	1101		1099	–	1108/1111	–	$65S_{25}$, $29S_{24}$	–	100	–
	ν_{26}	rCH_2 wag	1108	1051	5.5	0.05	0.75	1049		1046	–	1050/1054	–	$98S_{26}$	–	100	–
	ν_{27}	$=CH_2$ twist	1029	977	11.0	0.3	0.75	985		985	984	986/992	984	$61S_{27}$, $34S_{31}$	–	100	–
	ν_{28}	Ring deformation	959	931	9.4	15.4	0.75	900		896	896	899/902	903	$58S_{28}$, $12S_{32}$	–	100	–
	ν_{29}	$=CH_2$ rock	909	862	42.5	0.3	0.75	892		890	~886	894/899	888	$98S_{29}$	–	100	–
	ν_{30}	rCH_2 rock	864	830	4.6	5.7	0.75	816		814	816	811/815	816	$27S_{30}$, $35S_{28}$, $18S_{25}$, $15S_{24}$	–	100	–
	ν_{31}	=CH out-of-plane bend	686	656	4.7	3.7	0.75	663		663	–	674/676	–	$41S_{31}$, $30S_{27}$	–	100	–
	ν_{32}	Ring-C out-of-plane bend	319	316	1.3	6.7	0.75	308		–	315	323/324	325	$73S_{32}$	–	100	–
	ν_{33}	Asymmetric torsion	120	120	0.1	6.5	0.75	–		–	120	–	153	$90S_{33}$	–	100	–

[a] MP2(full)/6-31G(d) predicted values.
[b] MP2(full)/6-31G(d) fixed scaled frequencies with factors of 0.88 for CH stretches, 0.90 for heavy atom stretches and CH bends and 1.0 for all other modes.
[c] Scaled infrared intensities in km/mol from MP2(full)/6-31G(d).
[d] Scaled Raman activities in $Å^4$/u from MP2(full)/6-31G(d).
[e] Ref. [26]. For the gas the spectral region from 0 to 700, 800–1150, 1350–1400 and above 1700 were not reported; for the solid, spectral data for the regions 530–750, 1030–1160, and above 1650 were not reported; a dash indicates the regions which were omitted.
[f] Frequencies from Kr solution at −130 °C.
[g] Calculated with MP2(full)/6-31G(d) and contributions of less than 10% are omitted.
[h] *A*, *B* and *C* values in the last three columns are percentage infrared band contours.

Table 2
Observed and calculated frequencies (cm^{-1}) for *gauche* vinylcyclopropane

Vib. No.	Fundamental	Ab initio[a]	Fixed scaled[b]	IR int.[c]	Raman act.[d]	dp Ratio	IR gas	Raman gas[e]	IR Kr[f]	Raman liquid[e]	P.E.D.[g]	A[h]	B[h]	C[h]
ν_1	$=CH_2$ antisymmetric stretch	3310	3105	7.5	73.4	0.65	3098				$76S_1$, $22S_2$	22	72	6
ν_2	rCH_2 antisymmetric stretch	3307	3102	20.4	9.8	0.74					$75S_2$, $23S_1$	66	1	33
ν_3	$=CH_2$ symmetric stretch	3221	3022	3.2	179.5	0.09					$85S_3$	76	24	0
ν_4	rCH stretch	3200	3002	16.4	54.7	0.40					$72S_4$, $17S_6$	3	46	51
ν_5	rCH_2 symmetric stretch	3214	3015	5.6	8.3	0.10					$74S_5$, $17S_{22}$	63	35	2
ν_6	=CH stretch	3193	2995	13.5	58.9	0.69					$75S_6$, $20S_4$	32	58	10
ν_7	C=C stretch	1730	1642	8.7	13.4	0.21	1636	1638	1633	1639	$66S_7$, $16S_9$	95	5	0
ν_8	rCH_2 deformation	1570	1489	0.9	8.5	0.61					$79S_8$, $16S_{13}$	7	38	55
ν_9	$=CH_2$ deformation	1501	1425	4.5	17.7	0.34	1423	1426	1419	1419	$66S_9$, $12S_{12}$	0	84	16
ν_{10}	rCH in-plane bend	1444	1371	0.5	6.5	0.44			1375	1375	$42S_{10}$, $12S_8$, $11S_9$, $10S_{13}$	95	5	0
ν_{11}	=CH in-plane bend	1357	1288	0.7	11.7	0.41		1307	1310[h]		$62S_{11}$, $16S_7$, $12S_{15}$	81	13	6
ν_{12}	=C–C stretch	790	754	1.4	6.3	0.57	751	754	750[h]	752	$21S_{12}$, $34S_{18}$, $19S_{16}$, $14S_{17}$	1	83	16
ν_{13}	Ring breathing	1271	1207	2.7	14.4	0.21	1206	1203	1207	1199	$49S_{13}$, $23S_{10}$	100	0	0
ν_{14}	rCH_2 wag	1098	1043	9.2	0.6	0.20	1034				$73S_{14}$, $14S_{26}$	27	50	23
ν_{15}	$=CH_2$ wag	1130	1080	6.1	4.3	0.50	1075		~1075		$32S_{15}$, $10S_{13}$	88	6	6
ν_{16}	Ring deformation	995	959	8.8	9.8	0.72					$49S_{16}$, $12S_{12}$, $11S_{15}$	69	31	0
ν_{17}	rCH_2 rock	843	802	1.5	1.8	0.47					$58S_{17}$, $14S_{12}$	16	83	1
ν_{18}	rCH_2 twist	1158	1102	1.8	2.1	0.69	1091		~1089		$24S_{18}$, $20S_{10}$, $16S_{17}$	1	54	45
ν_{19}	C=C–C bend	538	525	0.1	2.1	0.65			527[h]	524	$43S_{19}$, $13S_{20}$, $10S_{15}$	1	86	13
ν_{20}	Ring-C in-plane bend	315	310	0.7	6.5	0.71					$40S_{20}$, $34S_{32}$	15	12	73
ν_{21}	rCH_2 antisymmetric stretch	3296	3092	0.6	73.8	0.74					$97S_{21}$	29	66	5
ν_{22}	rCH_2 symmetric stretch	3206	3008	13.2	67.5	0.14					$79S_{22}$, $15S_5$	20	71	9
ν_{23}	rCH_2 deformation	1524	1445	2.9	8.0	0.75					$99S_{23}$	1	93	6
ν_{24}	rCH_2 twist	1238	1175	1.5	9.3	0.74		1177	1173	1180	$42S_{24}$, $46S_{30}$, $10S_{25}$	28	60	12
ν_{25}	rCH out-of-plane bend	1177	1118	0.4	5.8	0.27					$53S_{25}$, $20S_{24}$	3	78	19
ν_{26}	rCH_2 wag	1113	1056	4.9	0.4	0.47					$83S_{26}$, $13S_{14}$	45	7	48
ν_{27}	$=CH_2$ twist	1036	983	21.2	0.8	0.21	991		993		$60S_{27}$, $30S_{31}$	10	5	85
ν_{28}	Ring deformation	954	925	5.2	14.9	0.70					$64S_{28}$, $18S_{15}$	2	28	70
ν_{29}	$=CH_2$ rock	934	886	37.5	0.1	0.67	913		~913		$98S_{29}$	13	0	87
ν_{30}	rCH_2 rock	871	834	6.5	4.4	0.73					$30S_{30}$, $18S_{25}$, $18S_{28}$, $16S_{24}$	18	77	5
ν_{31}	=CH out-of-plane bend	671	641	11.2	5.5	0.58	650		~650		$38S_{31}$, $28S_{27}$	11	3	86
ν_{32}	Ring-C out-of-plane bend	276	272	0.2	1.1	0.34					$31S_{32}$, $38S_{19}$, $25S_{20}$	78	21	1
ν_{33}	Asymmetric torsion	100	100	0.5	4.6	0.75					$90S_{33}$	77	19	4

[a] MP2(full)/6-31G(d) predicted values.
[b] MP2(full)/6-31G(d) fixed scaled frequencies with factors of 0.88 for CH stretches, 0.90 for heavy atom stretches and CH bends and 1.0 for all other modes.
[c] Scaled infrared intensities in km/mol from MP2(full)/6-31G(d).
[d] Scaled Raman activities in $Å^4/u$ from MP2(full)/6-31G(d).
[e] Ref. [26]. For the gas the spectral region from 0 to 700, 800–1150, 1350–1400 and above 1700 were not reported.
[f] Frequencies from Kr solution at –130 °C. Frequencies with an asterisk from Xe solution at −75 °C.
[g] Calculated with MP2(full)/6-31G(d) and contributions of less than 10% are omitted.
[h] A, B and C values in the last three columns are percentage infrared band contours.

Table 3
Calculated energies (hartree) and energy differences (cm^{-1}) for the stable *trans* and *gauche* conformers as well as the *cis* and *gauche'* transition states of vinylcyclopropane

Method/basis set	*Trans*	*Gauche* ΔE	*Cis* (TS) ΔE	*Gauche'* (TS) ΔE
RHF/6-31G(d)	−193.940214	469	912	1055
RHF/6-31+G(d)	−193.945565	506	942	1085
MP2/6-31G(d)	−194.604834	358	621	1042
MP2/6-31+G(d)	−194.617749	440	656	1055
MP2/6-311G(d,p)	−194.804386	401	529	1116
MP2/6-311+G(d,p)	−194.809074	437	546	1129
MP2/6-311G(2d,2p)	−194.858889	405	581	1213
MP2/6-311+G(2d,2p)	−194.862511	418	591	1237
MP2/6-311G(2df,2pd)	−194.938953	420	574	1244
MP2/6-311+G(2df,2pd)	−194.941895	440	586	1268
B3LYP/6-31G(d)	−195.291782	573	806	1242
B3LYP/6-31+G(d)	−195.300798	603	823	1228
B3LYP/6-311G(d,p)	−195.347045	571	820	1227
B3LYP/6-311+G(d,p)	−195.349090	581	824	1233
B3LYP/6-311G(2d,2p)	−195.355388	590	834	1249
B3LYP/6-311+G(2d,2p)	−195.357524	600	845	1261
B3LYP/6-311G(2df,2pd)	−195.361783	606	833	1272
B3LYP/6-311+G(2df,2pd)	−195.363731	616	844	1285

the infrared spectra were predicted by using the fixed scaled frequencies. Infrared intensities determined from MP2(full)/6-31G(d) calculations were calculated based on the dipole moment derivatives with respect to Cartesian coordinates. The derivatives were transformed with respect to normal coordinates by $(\partial\mu_u/\partial Q_i) = \sum_j (\partial\mu_u/\partial X_j)\ L_{ij}$, where Q_i is the ith normal coordinate, X_j is the jth Cartesian displacement coordinate, and L_{ij} is the transformation matrix between the Cartesian displacement coordinates and the normal coordinates. The infrared intensities were then calculated with $(N\pi)/(3c^2)$ $[(\partial\mu_x/\partial Q_i)^2 + (\partial\mu_y/\partial Q_i)^2 + (\partial\mu_z/\partial Q_i)^2]$. In Fig. 3C and D, the simulated infrared spectra of the pure *trans* and *gauche* conformers, are shown. The simulated spectra which was calculated at −130 °C, of the mixture of two conformers with a ΔH of 415 cm^{-1} is shown in Fig. 3B. It should be compared to the experimental spectrum of the krypton solution at −130 °C (Fig. 3A). The predicted spectrum is in remarkable resemblance to the experimental spectrum, indicating the utility of the scaled predicted data in distinguishing the fundamentals for the two conformers.

To further support the vibrational assignments, we have simulated the Raman spectra from ab initio MP2(full)/6-31G(d) results. The evaluation of Raman activity by using the analytical gradient methods has been developed [39,40]. The activity S_j can be expressed as: $S_j = g_j(45\alpha_j^2 + 7\beta_j^2)$, where g_j is the degeneracy of the vibrational mode j, α_j is the derivative of the isotropic polarizability, and β_j is that of the anisotropic polarizability. The Raman scattering cross sections, $\partial\sigma_j/\partial\Omega$, which are proportional to Raman activities, can be calculated from the scattering activities as well as the predicted wavenumbers for each normal mode, using the relationship [41,42]

$$\frac{\partial\sigma_j}{\partial\Omega} = \left(\frac{2^4\pi^4}{45}\right)\left(\frac{(\nu_0-\nu_j)^4}{1-\exp\left[\frac{-hc\nu_j}{kT}\right]}\right)\left(\frac{h}{8\pi^2 c\nu_j}\right)S_j$$

where ν_0 is the excitation wavenumber, ν_j is the vibrational wavenumber of the jth normal mode, and S_j is the corresponding Raman scattering activity. To obtain the polarized Raman scattering cross sections, the polarizabilities are incorporated into S_j by multiplying S_j with $(1-\rho_j)/(1+\rho_j)$, where ρ_j is the depolarization ratio of the jth normal mode. The Raman scattering cross sections and calculated wavenumbers obtained from the GAUSSIAN-03 program [36] were used together with a Lorentzian function to obtain the simulated Raman spectra.

The simulated Raman spectra of the pure *trans* and *gauche* conformers are shown in Fig. 5C and D, respectively. In Fig. 5B the mixture of the two conformers at 25 °C is shown utilizing the experimentally determined ΔH value of 415 cm^{-1} with the *trans* conformer the more stable form. The previously reported experimental Raman spectra of the liquid [26] at 23 and −120 °C are shown in Fig. 5A for comparison and the agreement between the simulated and the experimental spectra is considered satisfactory, but not nearly as good as that of the infrared spectra, probably due to the significant extent of intermolecular association in the liquid phase.

4. Vibrational assignment

In order to obtain the conformational stability it is necessary to assign the fundamentals correctly for the two different conformers. In the two previous Raman studies [25,26] only limited portions of the spectra were

Table 4
Structural parameters (Å and degree), rotational constants (MHz) and dipole moments (debye) for *trans* and *gauche* rotamers of vinylcyclopropane

Parameter	Internal coordinates	MP2(full)/6-311+G(d,p)		ED(*trans/gauche*)[a]		ED(*trans/gauche*)[b]			ED+MW[c]	MW[d]	Adjusted r_0[e]
		Trans	*Gauche*	I	II	I	II	III	*Trans*	*Trans*	*Trans*
$r(C_1–C_2)$	R_1	1.516	1.506	1.510	1.522	1.525(1)	1.521(1)	1.517(1)	1.521(4)	1.516(3)	1.521(5)
$r(C_1–C_3)$	R_2	1.516	1.517	1.510	1.522	1.525(1)	1.521(1)	1.517(1)	1.521(4)	1.516(3)	1.521(5)
$r(C_2–C_3)$	R_3	1.503	1.510	1.510	1.522	1.500	1.511	1.517	1.510(8)	1.509(3)	1.510(5)
$r(C_1–C_4)$	R_4	1.474	1.484	1.510	1.475	1.470(2)	1.466(2)	1.467(2)	1.481(7)	1.467(3)	1.474(5)
$r(C_4=C_5)$	R_5	1.343	1.342	1.334	1.334	1.336(1)	1.336(1)	1.336(1)	1.340(3)	1.344(3)	1.343(5)
$r(C_1–H_6)$	r_4	1.086	1.087	1.099	1.099	1.097(1)	1.099(1)	1.101(2)	1.098(3)	1.087[f]	1.086(3)
$r(C_4–H_7)$	r_3	1.091	1.090	1.099	1.099	1.097(1)	1.099(1)	1.101(2)	1.098(3)	1.087[f]	1.091(3)
$r(C_5–H_8)$	r_1	1.086	1.085	1.099	1.099	1.097(1)	1.099(1)	1.101(2)	1.098(3)	1.087[f]	1.086(3)
$r(C_5–H_9)$	r_2	1.084	1.085	1.099	1.099	1.097(1)	1.099(1)	1.101(2)	1.098(3)	1.087[f]	1.084(3)
$r(C_2–H_{10})$	r_5	1.084	1.083	1.099	1.099	1.097(1)	1.099(1)	1.101(2)	1.098(3)	1.087[f]	1.084(3)
$r(C_2–H_{11})$	r_6	1.084	1.083	1.099	1.099	1.097(1)	1.099(1)	1.101(2)	1.098(3)	1.087[f]	1.084(3)
$r(C_3–H_{12})$	r_7	1.084	1.084	1.099	1.099	1.097(1)	1.099(1)	1.101(2)	1.098(3)	1.087[f]	1.084(3)
$r(C_3–H_{13})$	r_8	1.084	1.084	1.099	1.099	1.097(1)	1.099(1)	1.101(2)	1.098(3)	1.087[f]	1.084(3)
$\angle C_1C_2C_3$		60.3	60.4						60.2(3)		60.3(5)
$\angle C_1C_3C_2$		60.3	59.7						60.2(3)		60.3(5)
$\angle C_2C_1C_3$		59.4	59.9						59.5(5)		59.4(5)
$\angle C_2C_1C_4$	θ_1	119.1	121.6	118.7(7)	120.1(9)				118.2(5)	119.3(2)	120.2(5)
$\angle C_3C_1C_4$	θ_2	119.1	119.3						118.2(5)	119.3(2)	120.2(5)
$\angle C_1C_4C_5$	ϕ_1	124.5	125.4	123.8(12)	126.2(14)	127.3(3)	127.6(3)	127.7(3)	125.8(6)	124.2(2)	123.6(5)
$\angle H_6C_1C_2$	ε_2	116.1	115.7						116.5[f]	118[f]	116.1(5)
$\angle H_6C_1C_3$	ε_3	116.1	114.5	116.8(15)	116.8(15)				116.5[f]	118[f]	116.1(5)
$\angle H_6C_1C_4$	ε_1	115.6	114.8	116.8(15)	116.8(15)	115.8[f]	115.8[f]	115.8[f]		118[f]	115.6(5)
$\angle H_7C_4C_5$	ϕ_3	119.4	118.8	119.7(15)	119.7(15)				116.8(25)	119.1[f]	119.4(5)
$\angle H_8C_5C_4$	γ_1	121.1	121.6	119.7(15)	119.7(15)	124.1(11)	124.8(11)	125.2(11)	117.8[f]	121.6[f]	121.1(5)
$\angle H_9C_5C_4$	γ_2	121.3	120.9	119.7(15)	119.7(15)				117.8[f]	121.6[f]	121.3(5)
$\angle H_{10}C_2C_3$	α_4	117.8	118.0	116.8(15)	116.8(15)				118.0(6)	114.1[f]	117.8(5)
$\angle H_{10}C_2C_1$	α_2	116.9	117.7	116.8(15)	116.8(15)				118.0(6)	114.1[f]	116.9(5)
$\angle H_{11}C_2C_3$	α_3	118.2	117.1	116.8(15)	116.8(15)					114.1[f]	118.2(5)
$\angle H_{11}C_2C_1$	α_1	117.5	118.0	116.8(15)	116.8(15)					114.1[f]	117.5(5)
$\angle H_{12}C_3C_2$	β_4	117.8	118.4	116.8(15)	116.8(15)				118.0(6)	114.1[f]	117.8(5)
$\angle H_{12}C_3C_1$	β_2	116.9	118.2	116.8(15)	116.8(15)				118.0(6)	114.1[f]	116.9(5)
$\angle H_{13}C_3C_2$	β_3	118.2	117.0	116.8(15)	116.8(15)					114.1[f]	118.2(5)
$\angle H_{13}C_3C_1$	β_1	117.5	116.5	116.8(15)	116.8(15)					114.1[f]	117.5(5)
$\tau H_6C_1C_4C_5$		0.0	126.9								
A		15124	11597							15076.2239(14)	15080
B		3058	3694							3061.4049(4)	3061
C		2942	3308							2941.3364(5)	2941
$\lvert\mu_a\rvert$		0.586	0.374								
$\lvert\mu_b\rvert$		0.000	0.137								
$\lvert\mu_c\rvert$		0.045	0.082								
$\lvert\mu_t\rvert$		0.587	0.407								

[a] Ref. [29].
[b] Ref. [24].
[c] Ref. [30].
[d] Ref. [28].
[e] This study.
[f] Assumed parameters.

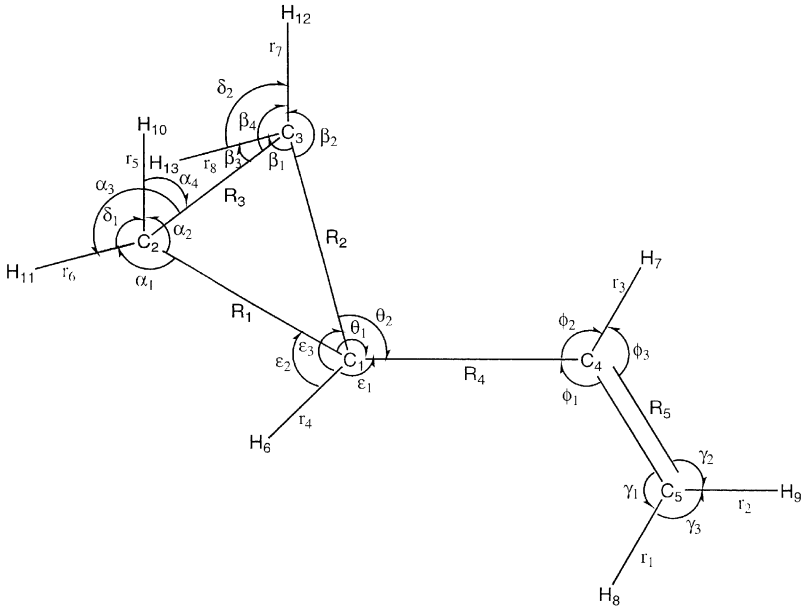

Fig. 4. The *trans* conformer of vinylcyclopropane with atom numbering and internal coordinates.

investigated and no attempt was made to provide a vibrational assignment. Since the most abundant conformer is the *trans* form with the plane of symmetry coinciding with the plane of *a* and *c* figure axes, the gas phase infrared band contours help immensely in making the assignment. All A″ modes will have pure B-type bands which makes them easily distinguishable. The predicted pure A-, B- and C-type contours in the IR are shown in Fig. 6 and those for the Raman Q-branches in Fig. 7. The ν_{31} fundamental provides an excellent example for this point since the *trans* conformer fundamental (A″) is predicted at 656 cm^{-1} with a pure B-type contour whereas the corresponding mode for the *gauche* conformer is predicted at 641 cm^{-1} with mainly a 11%A/84%C hybrid contour. There is no doubt on the correct assignment based on the observed contours (Fig. 7). Additionally, in one of the earlier Raman studies [26] a portion of the spectra of both the gas and solid were reported, for the *trans* form only the A′ modes should appear in the spectrum of the gas, all bands observed in the gas phase had corresponding lines in the solid, thus the *trans* conformer is the only form in the solid. Similarly, the infrared spectra of rare gas solutions and the solid along with the predicted frequencies and intensities for the fundamentals for both conformers from the ab initio MP2 (full)/6-31G(d) calculations make the assignment reasonably certain. Also, the infrared spectrum of the rare gas solution makes it possible to identify the band centers and separate closely spaced bands. By utilizing all of this information, practically all of the fundamentals of the *trans* conformer can be assigned confidently (Table 1). As an example, the *r*CH_2 (818 cm^{-1}) of A symmetry is predicted to have a lower frequency than the corresponding A mode (830 cm^{-1}). However, the band contours clearly show the A *r*CH_2 rock at 816 cm^{-1} whereas the corresponding A mode is observed. Assignment of several of the fundamentals for the *gauche* rotamer was made even though there is a relatively small amount of this conformer present at ambient temperature.

Initially, the fundamentals which were predicted to have significantly different values for the two conformers were identified when possible. As examples, the fundamentals between 400 and 1000 cm^{-1} are expected to be the most sensitive to conformational interchange and the predicted frequencies (with the observed values in parentheses) for the *trans* conformer are: 441 (446, ν_{19}), 656 (663, ν_{31}), 758 (761, ν_{18}), 818 (819, ν_{17}), 830 (816, ν_{30}), 862 (892, ν_{29}), 931 (900, ν_{28}), 969 (441, ν_{16}), and 985 (990, ν_{15}) cm^{-1}. Only three modes for the *gauche* conformer are expected to have higher frequencies than the corresponding *trans* modes and they are ν_{19}, ν_{29}, and ν_{30}, with predicted conformational frequency differences of 84, 24, and 4 cm^{-1}, respectively. The experimental differences of 86, 21, and 4 cm^{-1}, respectively, are in excellent agreement. The other six modes are predicted to have lower frequencies for the *gauche* form compared to the values for the corresponding vibrations for the *trans* form with predicted differences ranging from 2 to 16 cm^{-1}. The average predicted difference is 8 cm^{-1} and a 9 cm^{-1} average difference was observed. The largest difference between predicted and observed value is for ν_{18} with a predicted difference of 4 and an experimental value of 11 cm^{-1} (761 vs. 750 cm^{-1}). Thus, many of the fundamentals of the *gauche* conformer could be assigned even though there is a relatively small amount present. The assignment of the fundamentals for the *trans* conformer are listed in Table 1 and those for the *gauche* form in Table 2.

Table 5
Symmetry coordinates for *trans* vinylcyclopropane

Species	Description	Symmetry coordinate[a]
A′	$=CH_2$ antisymmetric stretch	$S_1 = r_1 - r_2$
	rCH_2 antisymmetric stretch	$S_2 = r_5 - r_6 + r_7 - r_8$
	$=CH_2$ symmetric stretch	$S_3 = r_1 + r_2$
	rCH stretch	$S_4 = r_4$
	rCH_2 symmetric stretch	$S_5 = r_5 + r_6 + r_7 + r_8$
	=CH stretch	$S_6 = r_3$
	C=C stretch	$S_7 = R_5$
	rCH_2 deformation	$S_8 = 4\delta_1 - \alpha_1 - \alpha_2 - \alpha_3 - \alpha_4 + 4\delta_2 - \beta_1 - \beta_2 - \beta_3 - \beta_4$
	$=CH_2$ deformation	$S_9 = 2\gamma_3 - \gamma_1 - \gamma_2$
	rCH in-plane bend	$S_{10} = 2\varepsilon_1 - \varepsilon_2 - \varepsilon_3$
	=CH in-plane bend	$S_{11} = \phi_2 - \phi_?$
	=C–C stretch	$S_{12} = R_4$
	ring breathing	$S_{13} = R_1 + R_2 + R_3$
	rCH_2 wag	$S_{14} = \alpha_1 + \alpha_2 - \alpha_3 - \alpha_4 + \beta_1 + \beta_2 - \beta_3 - \beta_4$
	$=CH_2$ wag	$S_{15} = \gamma_1 - \gamma_2$
	Ring deformation	$S_{16} = 2R_3 - R_1 - R_2$
	rCH_2 rock	$S_{17} = \alpha_1 - \alpha_2 + \alpha_3 - \alpha_4 + \beta_1 - \beta_2 + \beta_3 - \beta_4$
	rCH_2 twist	$S_{18} = \alpha_1 - \alpha_2 - \alpha_3 + \alpha_4 + \beta_1 - \beta_2 - \beta_3 + \beta_4$
	C=C–C bend	$S_{19} = \phi_1$
	Ring-C in-plane bend	$S_{20} = \theta_1 + \theta_2$
A″	rCH_2 antisymmetric stretch	$S_{21} = r_5 - r_6 - r_7 + r_8$
	rCH_2 symmetric stretch	$S_{22} = r_5 + r_6 - r_7 - r_8$
	rCH_2 deformation	$S_{23} = 4\delta_1 - \alpha_1 - \alpha_2 - \alpha_3 - \alpha_4 - 4\delta_2 + \beta_1 + \beta_2 + \beta_3 + \beta_4$
	rCH_2 twist	$S_{24} = \alpha_1 - \alpha_2 - \alpha_3 + \alpha_4 - \beta_1 + \beta_2 + \beta_3 - \beta_4$
	rCH out-of-plane bend	$S_{25} = \varepsilon_2 - \varepsilon_3$
	rCH_2 wag	$S_{26} = \alpha_1 + \alpha_2 - \alpha_3 - \alpha_4 - \beta_1 - \beta_2 + \beta_3 + \beta_4$
	$=CH_2$ twist	$S_{27} = \eta$
	Ring deformation	$S_{28} = R_1 - R_2$
	$=CH_2$ rock	$S_{29} = \kappa$
	rCH_2 rock	$S_{30} = \alpha_1 - \alpha_2 + \alpha_3 - \alpha_4 - \beta_1 + \beta_2 - \beta_3 + \beta_4$
	=CH out-of-plane bend	$S_{31} = \lambda$
	Ring-C out-of-plane bend	$S_{32} = \theta_1 - \theta_2$
	Asymmetric torsion	$S_{33} = \tau$

[a] Not normalized.

5. Conformational stability

There are only nine bands in the infrared spectrum of the gas which can be confidently assigned to the *gauche* conformer. These bands are also observed in the infrared spectrum of the krypton solution, but, practically all of them are shoulders on much more intense bands arising from fundamentals of the more stable *trans* conformer. In fact the only reasonably isolated bands in the infrared spectrum of the *gauche* conformer are the 650 cm^{-1} (Kr) band which is relatively pronounced, and the 751 cm^{-1} (Kr) (749 cm^{-1} in Xe) band which is relatively 'isolated' but very weak. These became the only two infrared bands of the *gauche* conformer which can be used for the conformational stability studies, except for the questionable 1325 cm^{-1} band which is presumably a combination band of the *gauche* conformer since it is not observed in the infrared spectrum of the solid. In the earlier Raman studies [25,26] the 1203 cm^{-1} line of the *gauche* form was used for the enthalpy studies since it is quite pronounced in the Raman spectrum. However, it is not useful for similar infrared studies since it is between two relatively strong infrared bands of the *trans* conformer as well as shoulders on both sides of the band. Therefore, only limited information can be obtained from the 1203 cm^{-1} band from the infrared spectrum. However, utilizing the weak band at 749 cm^{-1} for the *gauche* conformer along with three bands of the *trans* conformer with comparable intensities gave ΔH values ranging from a high value of 531 cm^{-1} to a low value of 365 cm^{-1} with an average of 460 cm^{-1}. Two additional conformer pairs were used (Table 6), which gave significantly lower values so the average ΔH value of the five pairs is 415 ± 16 cm^{-1}. Assuming 10% uncertainty rather than the statistical uncertainty from these determinations gives

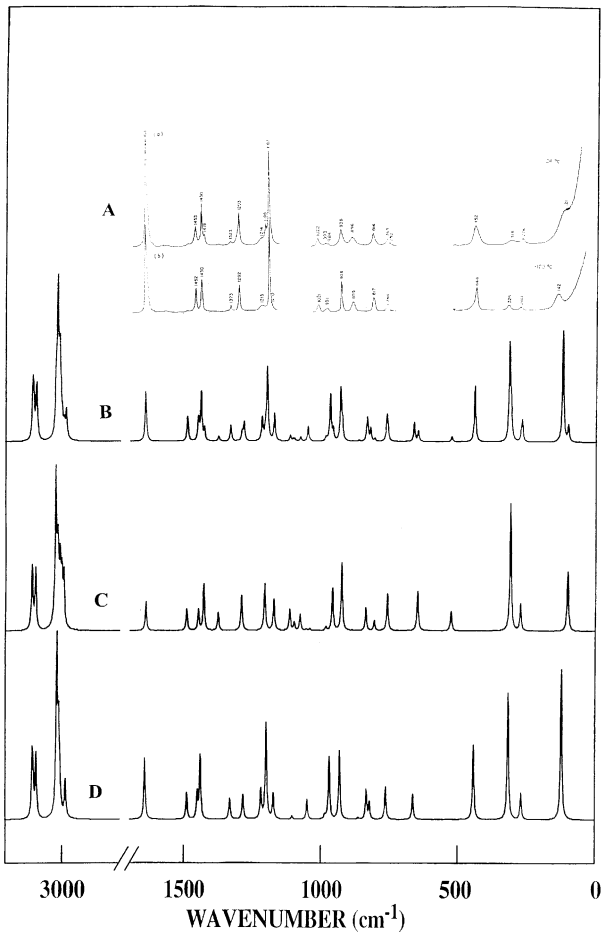

Fig. 5. Raman spectra of vinylcyclopropane: (A) liquid at 24 and −120 °C Ref. [25]; (B) simulated spectrum at 25 °C of a mixture of the two conformers with ΔH of 415 cm^{-1} with the *trans* form more stable; (C) simulated spectrum for pure *gauche* form; (D) simulated spectrum for pure *trans* form.

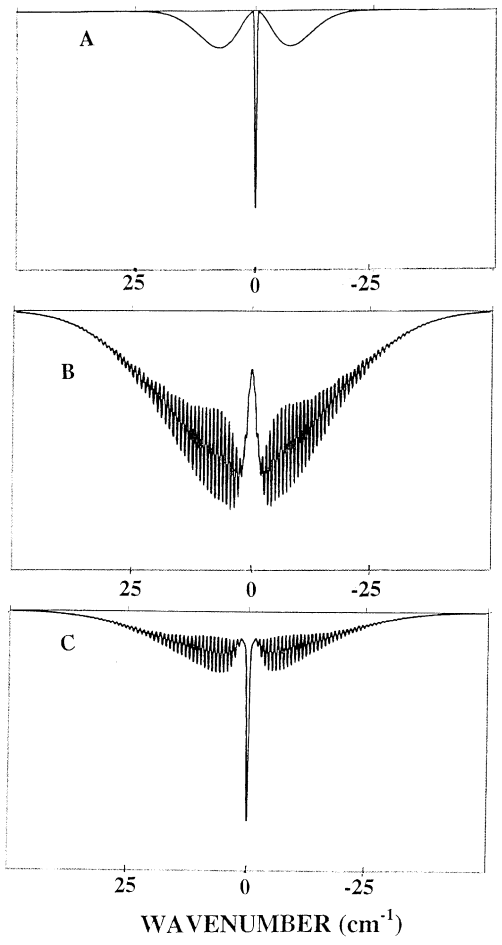

Fig. 6. Predicted pure A-, B- and C-type gas-phase infrared band contours for the *trans* and *gauche* conformers of vinylcyclopropane.

a value of $415 \pm 42\ cm^{-1}$ (4.96 ± 0.50 kJ/mol) for the experimental ΔH value from the infrared studies.

6. Structural parameters

We [43] have recently shown that ab initio MP2(full)/6-311+G(d,p) calculations predict the r_0 structural parameters for more than 50 carbon-hydrogen distances better than 0.002 Å compared to the experimentally determined [44] values from 'isolated' CH stretching frequencies. We have also found [35] that we can obtain good structural parameters by systematically adjusting the structural parameters obtained from the ab initio calculations to fit the rotational constants (computer program A&M, Ab initio and Microwave, developed in our laboratory) obtained from the microwave experimental data. In order to reduce the number of independent variables, the structural parameters are separated into several sets according to their type. Each set uses only one independent parameter in the optimization and all structural parameters in one set will be changed by the same adjustment factor. The information about the difference between similar structural parameters from ab initio calculations will be retained in the final results in the following way: bond lengths in the same set will keep their relative ratio and bond angles (including torsional angles) in the same set will keep their difference in degrees. This assumption is based on the fact that the errors from ab initio calculations are systematic which is commonly acknowledged. To avoid the possibility of falling into a local minimum instead of the global minimum, a simplex algorithm instead of a gradient method was used. The A&M program adds ab initio structural parameters, although with much smaller weights, to the rotational constants, so that the number of observable is always larger than the number of unknown parameters. As a consequence, unique results can be obtained without any arbitrary assumptions on the values of structural parameters.

The adjusted r_0 parameters for vinylcyclopropane are listed in Table 4 along with ab initio MP2(full)/6-311+G(d,p) predicted values. The fit of the previously reported [28] microwave rotational constants is given in Table 7 and the differences between the observed *B* and *C* values for five isotopomers and the fitted values is 0.3 MHz or less. The differences for the *A* moments is considerably higher but these constants have very large uncertainties.

7. Discussion

The enthalpy value of $415 \pm 42\ cm^{-1}$ from the rare gas solutions should be near the value in the gas phase [45–49] since the size and polarity of the two conformers are very similar. In the earlier Raman studies, two different enthalpy values were reported for the vapor from variable temperature studies of the 1191(*t*)/1203(*g*) cm^{-1} conformer pair with a low value [26] of $385 \pm 35\ cm^{-1}$ (4.61 ± 0.42 kJ/mol) and a high value [25] of $500 \pm 50\ cm^{-1}$. A smaller value had previously been reported [24] from the electron diffraction study. It was suggested [25] that the two different values probably arose from taking slightly different baselines as well as the spectral resolution used. Since it is possible to obtain the enthalpy difference from the previously reported spectra [25,26] at a single temperature by using the ab initio predicted Raman activities for this pair of lines, we calculated the enthalpy values for this conformer pair from both Raman studies (Fig. 7). For the Raman lines reported at the two different temperatures [26], enthalpy values of $377\ cm^{-1}$ (85 °C) and $392\ cm^{-1}$ (23 °C) were obtained, whereas the value obtained from the spectral data recorded [25] with a spectral slit width of $1\ cm^{-1}$ gave a value of $399\ cm^{-1}$. Both of these values support the lower value of $415\ cm^{-1}$ which we obtained from the variable temperature infrared spectra of the rare gas solutions. Also this lower value is in good agreement with the predicted values from the ab initio MP2 calculations with the largest value of $440\ cm^{-1}$ obtained with the 6–311+G(2df,2pd) basis set.

The vibrational assignment for the *trans* conformer could be made with confidence because of the band contours and

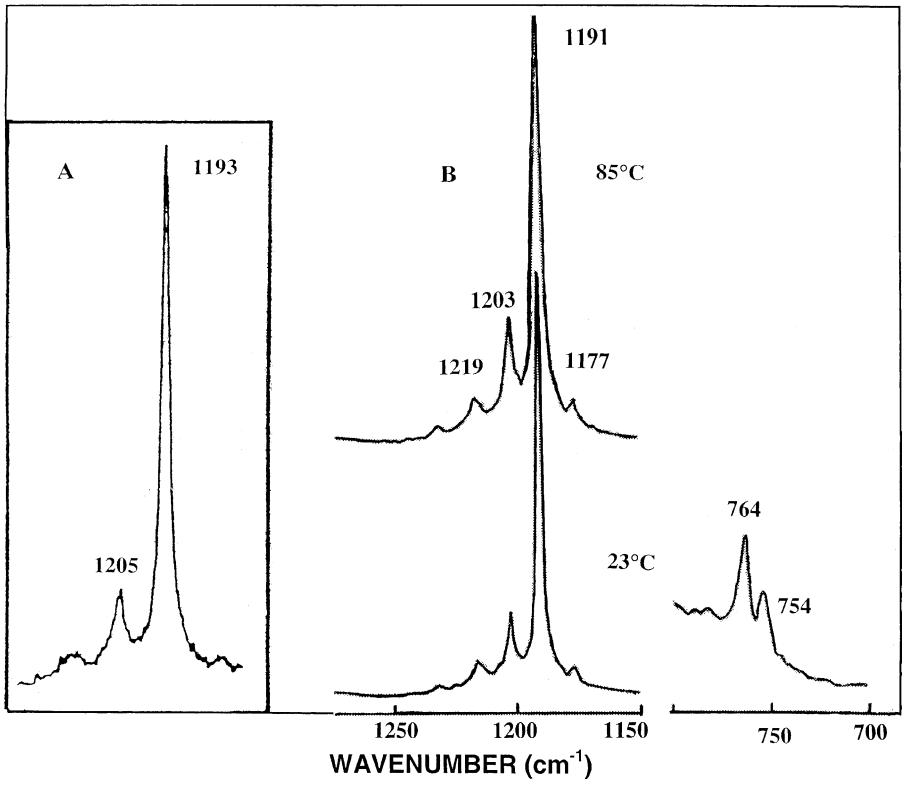

Fig. 7. Raman spectra of the vapor: (A) Ref. [25], and (B) Ref. [26].

the spectral data in the rare gas solutions and many of the fundamental for the *gauche* conformer could be identified. For those that not assigned it is assumed that they are in near coincidence with bands from the *trans* conformer. This is particularly true in the fingerprint region.

The adjusted r_0 parameters (Table 4) are very similar to the values obtained from the more recent electron diffraction study [24] where the microwave rotational constants were used as additional constraints. They are also within the values obtained from the more recent microwave study [28] if the listed uncertainties are taken into account. However, the results which we obtained in this study have confident values for the carbon-hydrogen distances as well as values for the angles.

The values for the structural parameters for the *gauche* conformer can be readily predicted by simply taking the predicted values from the MP2(full)/6-311+G(d,p) ab initio calculations and adjust them with the difference of the adjusted values of corresponding parameters from the *trans* conformer and the ab initio predicted values. For example the C_2–C_3 distance is predicted to be 0.007 Å longer in the *gauche* conformer than the corresponding bond distance for the *trans* form so this difference should be added to the adjusted value for this bond of the *trans*

Table 6
Temperature dependent intensity ratios for the *trans* and *gauche* conformers of vinyl cyclopropane dissolved in liquid xenon

T (°C)	$1000/T$ (K^{-1})	I_{440t}/I_{749g}	I_{761t}/I_{749g}	I_{1321t}/I_{749g}	I_{440t}/I_{1325g}	I_{761t}/I_{1325g}	I_{1321t}/I_{1325g}
−55.0	4.5840	1.22001	3.12606	2.21145	0.54734	1.40247	0.99214
−60.0	4.6915	1.36471	3.48896	2.25743	0.62118	1.58808	1.02752
−65.0	4.8042	1.50883	3.85698	2.38500	0.67344	1.72148	1.06449
−70.0	4.9225	1.63089	4.42706	2.64297	0.68610	1.86242	1.11187
−75.0	5.0467	1.80467	4.55784	2.72697	0.75623	1.90992	1.14271
−80.0	5.1773	2.20746	5.38140	3.04928	0.87158	2.12475	1.20395
−85.0	5.3149	2.04365	5.50212	3.08542	0.82223	2.21370	1.24138
−90.0	5.4600	2.21247	6.31863	3.40779	0.84530	2.41411	1.30198
−95.0	5.6132	2.55778	7.13498	3.74458	0.92843	2.58987	1.35921
−100.0	5.7753	2.96193	7.93111	4.08111	1.02399	2.74192	1.41091
ΔH (cm^{-1})	Individual pair	482±33	531±19	365±12	325±32	373±19	208±4
Linearity coefficient (R^2)		0.9629	0.9901	0.9910	0.9300	0.9803	0.9975
ΔH (cm^{-1})	Statistical average	381±17 (*trans* conformer more stable)					

Table 7
Comparison of rotational constants obtained from modified ab initio, MP2/6-311+G(d,p) structural parameters and those from microwave spectra for *trans*-vinylcyclopropane

Isotopomer	Rotational constants (MH_Z)	Observed[a]	Calculated	Δ
c-($^{12}CH_2^{12}CH_2^{12}$ CH)$^{12}CH{=}^{12}CH_2$	*A*	15076.2	15080.0	3.8
	B	3061.4	3061.5	0.1
	C	2941.4	2941.4	0.0
c-($^{13}CH_2^{12}CH_2^{12}$ CH)$^{12}CH{=}^{12}CH_2$	*A*	14821(7)	14832.3	11.3
	B	3022.7	3022.6	−0.1
	C	2896.5	2896.2	−0.3
c-($^{12}CH_2^{12}CH_2^{13}$ CH)$^{12}CH{=}^{12}CH_2$	*A*	15014(15)	15006.5	−7.5
	B	3057.2	3057.5	0.3
	C	2940.6	2940.5	−0.1
c-($^{12}CH_2^{12}CH_2^{12}$ CH)$^{13}CH{=}^{12}CH_2$	*A*	15016.3(9)	15010.8	−5.5
	B	3041.1	3040.9	−0.2
	C	2925.1	2924.9	−0.2
c-($^{12}CH_2^{12}CH_2^{12}$ CH)$^{12}CH{=}^{13}CH_2$	*A*	15075(6)	15073.0	−2.0
	B	2972.9	2973.1	−0.2
	C	2859.8	2860.0	0.2

[a] Values for the rotational constants taken from Ref. [28].

conformer. From these parameters it should be relatively easy to assign the rotational spectrum arising from the *gauche* conformer.

In one of the earlier Raman studies [26] the spectra of the solid were reported where two significantly different reproducible spectra were observed. The spectra were assigned to two crystal forms, which were attributed to the rate of cooling. Also, these authors suggested that the differences in the spectra were probably due to differences in the crystal packing. We initially expected that the spectrum of the solid which had a good correspondence [26] with the spectrum of the liquid could have been mainly due to annealing with the sample being more like an amorphous solid. Therefore, we reinvestigated the vibrational spectra of vinylcyclopropane utilizing the infrared spectrum of the sample on a flat plate, which makes the annealing considerably easier since the temperature can be more easily controlled and the sample can be continuously observed. The results of these studies are shown in Fig. 9 and it is clear that the initially obtained spectrum is in fact

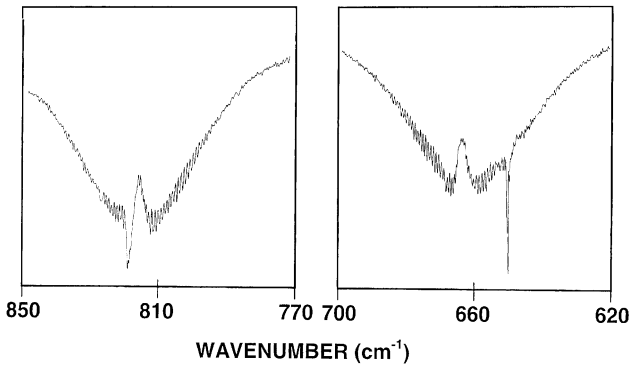

Fig. 8. Infrared spectra of vinylcyclopropane showing the band contours.

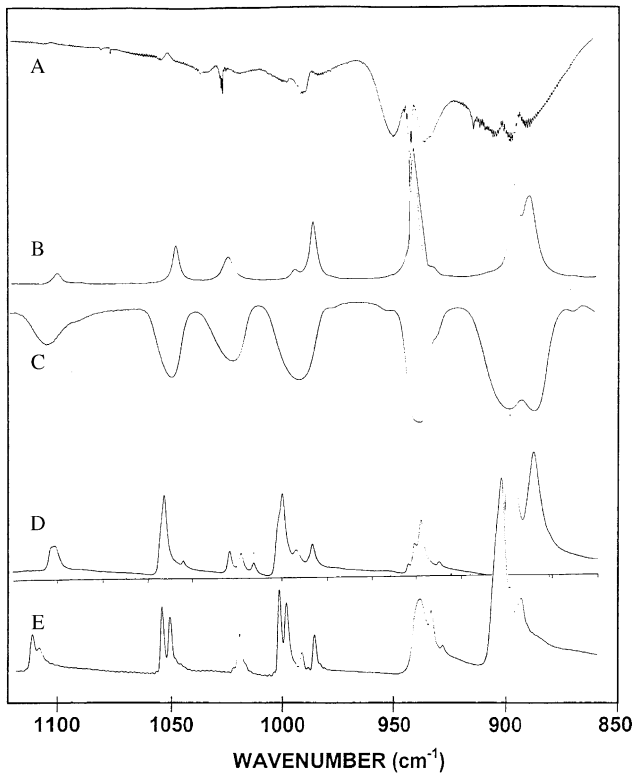

Fig. 9. Mid-infrared spectra (850–1120 cm^{-1}) of vinylcyclopropane: (A) gas; (B) krypton solution; (C) amorphous solid; (D) first annealed solid; (E) second annealed solid.

quite crystalline and has at least four molecules per primitive cell since several of the fundamentals split into four peaks with many of them observed in both the infrared and Raman spectra. However, by repeated additional annealing many of the peaks disappear leaving two well-defined bands for most of the fundamentals.

A single-crystal X-ray study [50,51] has been reported for vinylcyclopropane with the measurements made at 94 K. In addition to the conventional full-angle refinements ($\sin\theta/\lambda < 1.22$ Å^{-1}) higher-order refinements ($\sin\theta/\lambda < 0.70$ Å^{-1}) were performed to obtain accurate parameters for the C atoms [51]. For the full angle refinement on 3480 observed independent reflections it was found that the molecules in the crystal deviated slightly from the *trans*-bisected conformation in a monoclinic $P2_1$ (D_2^2) cell [$a=4.879(1)$, $b=7.161(1)$, $c=6.923(1)$] and $Z=2$. The two molecules must occupy the two C_1 sites and one, therefore, expects each fundamental to be a doublet from the factor group with the Raman and infrared bands having the same frequencies. Since the molecular symmetry is C_s with both the A′ and A″ modes being active in both the infrared and Raman spectra, the lower C_1 symmetry of the site will not affect the vibrational spectrum. However, the skeletal movement from the symmetry plane for the molecule in the fluid phases to the crystal should affect the vibrations, which are the most sensitive to the molecular conformation. An inspection of the data in Tables 1 and 2 shows significant

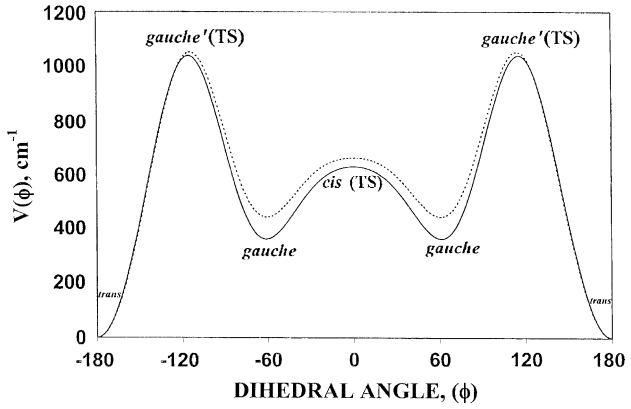

Fig. 10. Calculated potential functions governing asymmetric torsion in vinylcyclopropane. Solid curve from MP2(full)/6-31G(d) and dotted curve from MP2(full)/6-31+G(d) calculations. Dihedral angle 180° defined for the *trans* conformer.

frequency differences for ν_{12} which is predicted to be 10 cm^{-1} higher for the *gauche* form as well as the out-of-phase $r$$CH_2$ wag (ν_{26}). Therefore, the observed shifts of the bands between the two observed infrared spectra of the two solids as well as the Raman spectra of the two different crystals appears to be consistent with the initially obtained spectrum being due to four molecules with C_s symmetry per primitive cell. The second crystal phase gives spectral data consistent with the published crystal structure with the partially rotated heavy atom frame, which destroys the molecular plane of symmetry. (Fig. 9)

The asymmetric torsional potential governing conformational interchange has been predicted from ab initio calculations. Beginning at the global minimum for the most stable *trans* conformer (dihedral 180°), the potential function was determined by rotating the vinyl moiety at increments of 15° throughout a 360° cycle. The energies were calculated with full optimization of all structural parameters, except for the varying dihedral angle, at each point from both MP2(full)/6-31G(d) and MP2(full)/6-31+G(d) calculations. The doubly degenerate *gauche* conformers appear as minima on the plot, with skeletal dihedral angles of $\sim\pm60°$. The local maximum at dihedral 0° assumes the *cis* orientation while the two doubly degenerate *gauche'* transition states (global maxima) assume $\sim\pm115°$ dihedral angle. The *trans*-to-*gauche* barrier (via *gauche'* maxima) was predicted to be 1042 cm^{-1} from MP2(full)/6-31G(d) level and slightly higher at 1055 cm^{-1} from MP2(full)/6-31+G(d) level, whereas the *gauche*-to-*gauche* barrier (via *cis* maximum) was predicted to be only 263 and 216 cm^{-1}, respectively (Table 6). The calculated potential functions are shown in Fig. 10. By fitting a Fourier cosine series to represent the asymmetric potential function with the form $V(\phi)=\sum_{i=1}^{6}(V_i/2)(1-\cos i\phi)$, the potential constants for the first six cosine terms were obtained. All predicted potential constants with the exception of the V_1 terms agree reasonably well between the two levels of calculation. These potential constants, fitted from MP2(full)6-31G(d) and MP2(full)6-31+G(d) results, are listed in Table 8.

The potential constants determined by fitting the observed two quantum jumps in the Raman spectrum of the gas [25] are also listed in Table 8. The major differences are the much larger values for the V_2 and V_4 terms compared to the predicted values. Also it should be noted that the *gauche*-to-*gauche* barrier is more than twice the predicted ones. These investigators [25] also obtained the potential constants by using the smaller ΔH value from the other Raman study [26] where the most significant difference is the V_1 term. These experimental results clearly indicate a much different frequency separations should be found for the *gauche* excited torsional states from those predicted from the ab initio calculations. Unfortunately, no experimental information is available on the torsional excited state frequencies for the *gauche* conformer which could be used to obtain more definitive information on the *gauche* well.

Table 8
Calculated potential barriers and Fourier potential coefficients of vinylcyclopropane

Coefficients (cm^{-1})	MP2(full)/6-31G(d)	MP2(full)/6-31+G(d)	Ref. [25]	Ref. [26]
V_1	−60	−131	−279±60	−111
V_2	396	439	699±60	752
V_3	−652	−613	−782±32	−784
V_4	111	103	−199±35	−203
V_5	81	81	–	–
V_6	−14	−15	–	–
ΔE	358	440		
ΔH			500	385
Potential barriers (cm^{-1})				
Trans→*gauche*	1042	1055	1373	1361
Gauche→*trans*	684	615	877	980
Gauche→*gauche*	263	216	564	514
Gauche dihedral angle				
Gauche (min)	60.5°	60.1°		
Gauche' (max)	116.0°	114.8°		

Acknowledgements

JRD acknowledges the University of Kansas City Trustees for a Faculty Fellowship award for partial financial support of this research.

References

[1] C.J. Wurrey, Y.Y. Yeh, M.D. Weakly, V.F. Kalasinsky, J. Raman Spectrosc. 15 (1984) 179.
[2] C.J. Wurrey, S. Shen, X. Zhu, H. Zhen, J.R. Durig, J. Mol. Struct. 449 (1998) 203.
[3] W. Caminati, R. Danieli, M. Dakkouri, R. Bitschenauer, J. Phys. Chem. 99 (1995) 1867.
[4] G.A. Guirgis, C.J. Wurrey, Z. Yu, X. Zhu, J.R. Durig, J. Phys. Chem. A 103 (1999) 1509.
[5] J.R. Durig, S.E. Godbey, S.A. Faust, J. Mol. Struct. 176 (1988) 123.
[6] V.F. Kalasinsky, C.J. Wurrey, J. Raman Spectrosc. 9 (1980) 315.
[7] F.G. Fujiwara, J.C. Chang, H. Kim, J. Mol. Struct. 41 (1977) 177.
[8] M.A. Mohammadi, W.V.F. Brooks, J. Mol. Spectrosc. 77 (1979) 42.
[9] C.J. Wurrey, R. Krishnamoorthi, S. Pechsiri, V.F. Kalasinsky, J. Raman Spectrosc. 12 (1982) 95.
[10] C.J. Wurrey, Y.Y. Yeh, R. Krishnamoorthi, R.J. Berry, J.E. DeWitt, V.F. Kalasinsky, J. Phys. Chem. 88 (1984) 4059.
[11] J.R. Durig, S. Shen, X. Zhu, C.J. Wurrey, J. Mol. Struct. 485/486 (1999) 501.
[12] J.R. Durig, Z. Yu, C. Zheng, G.A. Guirgis, J. Phys. Chem. A 108 (2004) 5353.
[13] N. Inamoto, S. Masuda, Chem. Lett. (1982) 1003.
[14] J.R. Durig, S. Shen, W. Zhao, L. Zhou, Chem. Phys. 213 (1996) 165.
[15] J.R. Durig, A. Wang, T.S. Little, J. Mol. Struct. 244 (1991) 117.
[16] J.R. Durig, H.D. Bist, T.S. Little, J. Chem. Phys. 61 (1988) 529.
[17] J.R. Durig, S. Shen, W. Zhao, L. Zhou, J. Mol. Struct. 407 (1997) 11.
[18] K.P.R. Nair, J.E. Boggs, J. Mol. Struct. 33 (1976) 45.
[19] H.N. Volltrauer, R.H. Schwendenman, J. Chem. Phys. 54 (1971) 268.
[20] L.S. Bartell, J.P. Guillory, A.T. Parks, J. Phys. Chem. 69 (1965) 3043.
[21] J.R. Durig, S. Shen, Spectrochim. Acta A 56 (2000) 2545.
[22] H.D. Volltrauer, R.H. Schwendenman, J. Chem. Phys. 54 (1971) 260.
[23] L.S. Bartell, J.P. Guillory, J. Chem. Phys. 43 (1965) 647.
[24] A. de Meijere, W. Lüttke, Tetrahedron 25 (1969) 2047.
[25] L.A. Carrerra, T.G. Towns, T.B. Malloy Jr., J. Am. Chem. Soc. 100 (1978) 385.
[26] V.R. Salares, W.F. Murphy, H.J. Bernstein, J. Raman Spectrosc. 7 (1978) 147.
[27] E.G. Codding, R.H. Schwendeman, J. Mol. Spectrosc. 49 (1974) 226.
[28] Z. Kisiel, P.W. Fowler, A.C. Legon, P. Dixneuf, J. Chem. Soc. Faraday Trans. 92 (1996) 906.
[29] M. Traetteberg, P. Bakken, J. Mol. Struct. 189 (1988) 357.
[30] Q. Shen, M. Traetteberg, J. Mol. Struct. 654 (2003) 162.
[31] J.X. Hou, M.B. Huang, J. Mol. Struct. 585 (2002) 93.
[32] B. Klahn, V. Dyczmons, J. Mol. Struct. 122 (1985) 75.
[33] M.B. Huang, D.K. Pan, J. Mol. Struct. 108 (1984) 49.
[34] G.R. de Mare, M.R. Peterson, J. Mol. Struct. 89 (1982) 213.
[35] B.J. van der Veken, W.A. Herrebout, D.T. Durig, W. Zhao, J.R. Durig, J. Phys. Chem. A 103 (1999) 1976.
[36] M.J. Frisch, G.W. Trucks, H.B. Schlegel, G.E. Scuseria, M.A. Robb, J.R. Cheeseman, J.A. Montgomery Jr., T. Vreven, K.N. Kudin, J.C. Burant, J.M. Millam, S.S. Iyengar, J. Tomasi, V. Barone, B. Mennucci, M. Cossi, G. Scalmani, N. Rega, G.A. Petersson, H. Nakatsuji, M. Hada, M. Ehara, K. Toyota, R. Fukuda, J. Hasegawa, M. Ishida, T. Nakajima, Y. Honda, O. Kitao, H. Nakai, M. Klene, X. Li, J.E. Knox, H.P. Hratchian, J.B. Cross, C. Adamo, J. Jaramillo, R. Gomperts, R.E. Stratmann, O. Yazyev, A.J. Austin, R. Cammi, C. Pomelli, J.W. Ochterski, P.Y. Ayala, K. Morokuma, G.A. Voth, P. Salvador, J.J. Dannenberg, V.G. Zakrzewski, S. Dapprich, A.D. Daniels, M.C. Strain, O. Farkas, D.K. Malick, A.D. Rabuck, K. Raghavachari, J.B. Foresman, J.V. Ortiz, Q. Cui, A.G. Baboul, S. Clifford, J. Cioslowski, B.B. Stefanov, G. Liu, A. Liashenko, P. Piskorz, I. Komaromi, R.L. Martin, D.J. Fox, T. Keith, M.A. Al-Laham, C.Y. Peng, A. Nanayakkara, M. Challacombe, P.M.W. Gill, B. Johnson, W. Chen, M.W. Wong, C. Gonzalez, J.A. Pople, GAUSSIAN 03, Revision B.04, Gaussian, Inc., Pittsburgh, PA, 2003.
[37] P. Pulay, Mol. Phys. 179 (1969) 197.
[38] G.A. Gurigis, X. Zhu, Z. Yu, J.R. Durig, J. Phys. Chem. A 104 (2000) 4383.
[39] M.J. Frisch, Y. Yamaguchi, J.F. Gaw, H.F. Schaefer III, J.S. Binkley, J. Chem. Phys. 84 (1986) 531.
[40] R.D. Amos, Chem. Phys. Lett. 124 (1986) 376.
[41] P.L. Polavarapu, J. Phys. Chem. 94 (1990) 8106.
[42] G.W. Chantry, in: A. Anderson (Ed.), The Raman Effect, vol. 2, Marcel Dekker, New York, 1971 (Chapter 2).
[43] J.R. Durig, K.W. Ng, C. Zheng, S. Shen, Struct. Chem. 15 (2004) 149.
[44] D.C. McKean, J. Mol. Struct. 113 (1984) 251.
[45] W.A. Herrebout, B.J. van der Veken, J. Phys. Chem. 100 (1996) 9671.
[46] W.A. Herrebout, B.J. van der Veken, A. Wang, J.R. Durig, J. Phys. Chem. 99 (1995) 578.
[47] M.O. Bulanin, J. Mol. Struct. 347 (1995) 73.
[48] B.J. van der Veken, F.R. DeMunck, J. Chem. Phys. 97 (1992) 3060.
[49] M.O. Bulanin, J. Mol. Struct. 19 (1973) 59.
[50] D. Nijveldt, A. Vos, Acta Crystallogr. B44 (1988) 281.
[51] D. Nijveldt, A. Vos, Acta Crystallogr. B44 (1988) 296.